Inorganic Chemistry
Cite This: Inorg. Chem. 2019, 58, 3302−3307
Article
pubs.acs.org/IC

# $Ba_3CrN_3H$: A New Nitride-Hydride with Trigonal Planar $Cr^{4+}$

Nathaniel W. Falb,[†,‡] Jennifer N. Neu,[†,‡] Tiglet Besara,*[,†,§] Jeffrey B. Whalen,[†] David J. Singh,[∥] and Theo Siegrist[†,⊥]

[†]National High Magnetic Field Laboratory, Tallahassee, Florida 32310, United States
[‡]Department of Physics, Florida State University, Tallahassee, Florida 32306, United States
[§]Department of Physics, Astronomy, and Materials Science, Missouri State University, Springfield, Missouri 65897, United States
[∥]Department of Physics and Astronomy, University of Missouri-Columbia, Columbia Missouri 65211, United States
[⊥]Department of Chemical and Biomedical Engineering, FAMU-FSU College of Engineering, Tallahassee, Florida 32310, United States

**ABSTRACT:** The nitride-hydride $Ba_3CrN_3H$ was obtained in single crystalline form using flux growth techniques based on alkaline earth metals. $Ba_3CrN_3H$ crystallizes in the hexagonal space group $P6_3/m$ (Nr 176), with the lattice parameters $a$ = 8.0270(2) Å, $c$ = 5.6240(1) Å, and $Z$ = 2. The structure comprises $[CrN_3]^{5-}$ trigonal planar units and $[HBa_6]^{11+}$ octahedral units. The presence of anionic hydrogen in the structure has been verified by $^1$H NMR experiments. DFT calculations show that the addition of hydrogen increases the stability of the phase versus $Ba_3CrN_3$. The two d-electrons of $Cr^{4+}$ are located in the nonbonding $d_{z^2}$ orbital, rendering $Ba_3CrN_3H$ nonmagnetic and insulating.

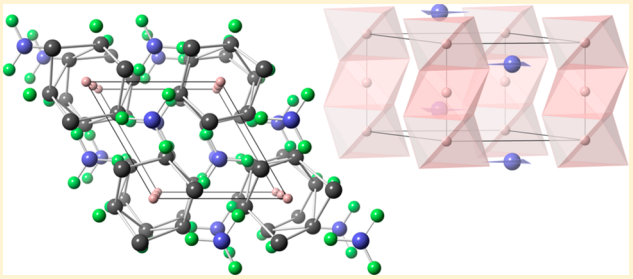

## INTRODUCTION

Of the mixed anionic compounds that contain both hydrogen and nitrogen, only a few are known. Among these, $Li_4NH$ has been studied in more details.[1−5] Additionally, the nitride-hydrides of the alkaline earth metals calcium,[6] strontium,[7] and barium[7] have been reported. Quaternary compounds that combine anionic nitrogen and anionic hydrogen are also quite rare. The first one, $Ca_6Cr_2N_6H$, was described only recently.[8] Other quaternary systems, based on the combination of lithium and alkaline earth nitride-hydrides, such as $LiSr_2H_2N$ have been described in the literature.[1]

In $Ca_6Cr_2N_6H$, the transition element Cr is in planar three-coordination by nitrogen, whereas the hydrogen is found bonded to the alkaline earth calcium exclusively. The hydrogen atom is at the center of a distorted calcium octahedron, isolating it well from the $CrN_3$ units. Two Cr atoms link up and are present as $Cr^{4+}$ and $Cr^{3+}$, as corroborated by susceptibility measurements.[8] In another system described recently, $Ca_3SiN_3H$, $SiN_4$ tetrahedra link up via corners to form linear chains, while the hydrogen anion is again coordinated by six calcium ions.[9] The hydrogen affinity of alkaline earth metals, in these cases calcium that is abundant in these structures, serves to provide an environment for structurally isolating hydrogen from other metals. Thus, one would expect that nitride-hydrides might form in alkali and alkaline earth rich compounds that accommodate both hydrogen and nitrogen. In the case of quaternary compounds, the alkaline and alkaline earths coexist with another ion, such as a (high-valent) transition metal, or a main group metal, such as Si, so that nitrogen atoms can complete a coordination polyhedron around the transition metal.

We have investigated molten barium and barium/magnesium fluxes for their ability to simultaneously dissolve multiple anions, leading to new compounds such as $Ba_2TeO$, $Ba_3Ln_2O_5Cl_2$ (Ln = Gd to Lu), and $Ba_3Yb_2O_5Te$.[10−12] Since nitrides as well as hydrides are soluble in molten alkaline earth fluxes, we attempted to synthesize novel phases combining anionic nitrogen and hydrogen. In one of our reactions, greenish crystals with hexagonal habit were found, with composition $Ba_3CrN_3H$.[13]

## METHODS

All samples measured were prepared (grown) utilizing a molten metal flux technique. A 9:1 Ba:Mg ratio was exploited in order to allow the growth to occur at lower temperatures. In an inert environment, stainless steel tubing was loaded with freshly cut barium metal pieces (27 mmol), magnesium turnings (3 mmol), barium hydride powder (1 mmol), and chromium nitride powder (2 mmol). The stainless steel tube was then welded shut, and sealed in an evacuated quartz ampule. The ampule was heated to 1000 °C in 10 h, held at 1000 °C for 24 h, then cooled slowly down to 850 °C in 150 h (1 °C/h). Once this temperature was reached, the reaction was removed from the furnace while the flux was still molten (the 9:1 Ba:Mg ratio solidifies at ∼630 °C), inverted, and centrifuged to allow proper separation of crystals from the flux. During the centrifugation, the flux solidifies on one end of the tube while the crystals reside on the other end,

Received: December 3, 2018
Published: February 14, 2019






DOI: 10.1021/acs.inorgchem.8b03367
Inorg. Chem. 2019, 58, 3302−3307

allowing for easy harvesting after cutting open the stainless-steel tube (in an inert atmosphere).

Energy-dispersive spectroscopy (EDS), using a Zeiss Scanning Electron Microscope with an acceleration voltage of 25 kV, was used to determine the presence of Ba, Cr, and N, and to confirm the 3:1 Ba/Cr ratio.

Structural characterization of the new phase was carried out using an Oxford Diffraction Xcalibur-2 CCD diffractometer with graphite-monochromatized Mo K$\alpha$ radiation. The crystals are highly reactive and degrade under ambient conditions within a short time and were therefore mounted in cryoloops under Paratone-N oil and cooled to 200 K. In this way, their integrity was ensured; no degradation was observed during data collection. Data were collected using $\omega$ scans with 1° frame widths to a resolution of approximately 0.39 Å, equivalent to $2\theta \approx 133°$. Reflections were recorded, indexed, and corrected for absorption using the Rigaku Oxford Diffraction CrysAlisPro software,[14] and subsequent calculations were carried out using the X-ray structure refinement and analysis software CRYSTALS,[15] employing Superflip[16] to solve the crystal structure. The data quality allowed for an unconstrained full-matrix refinement against $F^2$, with anisotropic thermal displacement parameters for all non-hydrogen atoms and with isotropic thermal displacement parameters for the hydrogen. The hydrogen was manually placed based on theoretical calculations (see below). Crystallographic information files have been deposited with the Inorganic Crystal Structure Database[17] via the Cambridge Structural Database[18] (CCDC 1874911 for a crystal with data collected at 100 K, and CCDC 1879699 for a crystal with data collected at 200 K). Diffraction and crystallography parameters are summarized in Tables 1 and 2 for the 200 K data collection.

**Table 1. Single Crystal X-ray Diffraction Data and Collection Parameters for a Collection at 200 K (CCDC 1879699)**

| | $Ba_3CrN_3H$ |
|---|---|
| molecular weight | 507.04 g/mol |
| space group | $P6_3/m$ (#176) |
| $a$ | 8.0270(2) Å |
| $c$ | 5.6241(1) Å |
| $Z$ | 2 |
| $V$ | 313.83(1) Å$^3$ |
| $\rho_{calc}$ | 5.366 g/cm$^3$ |
| $\mu$ | 20.132 mm$^{-1}$ |
| data collection range | $2.93° < \theta < 66.51°$ |
| reflections collected | 14499 |
| independent reflections | 1972 |
| parameters refined | 16 |
| $R_1$ | 0.0447 |
| $wR_2$ | 0.0555 |
| goodness-of-fit on $F^2$ | 0.9995 |

**Table 2. Atomic Positions of $Ba_3CrN_3H$ (CCDC 1879699)**

| atom | site | $x$ | $y$ | $z$ | $U_{eq}$ (Å$^2$) |
|---|---|---|---|---|---|
| Ba | 6h | 0.34825(3) | 0.26115(3) | 1/4 | 0.0065(6) |
| Cr | 2c | 1/3 | 2/3 | 1/4 | 0.0042(2) |
| N | 6h | 0.1245(5) | 0.4430(4) | 1/4 | 0.0087(9) |
| H | 2b | 0 | 0 | 0 | 0.0100 ($U_{iso}$) |

The samples were checked for the presence of hydrogen by means of $^1$H solid-state nuclear magnetic resonance (NMR) ($I = 1/2$, $\gamma/2\pi = 42.5774$ MHz/T) using an NMR spectrometer locally developed at the National High Magnetic Field Laboratory. Spectra were obtained with the free induction decay method at $T = 100$ K. Due to the relatively narrow $^1$H spectrum width compared to the spectrometer bandwidth, there was no need to sweep the field or the frequency, and pulsing at a fixed frequency was enough to obtain the full hydrogen spectrum. In order to minimize the contribution from the ubiquitous presence of hydrogen in insulation materials and probe assembly parts, a Teflon-insulated silver wire was used to make a coil for the sample holder since the more commonly used copper wire is insulated with a polymer. In addition, a piece of Teflon tubing wrapped in Teflon tape was used as sample holder. The whole coil−holder−sample setup was mounted with extra long leads (~3 cm) in order for the sample to be as far away from other parts of the probe as possible. Furthermore, to unambiguously determine whether the $^1$H signal was from the sample, two identical sample holders were prepared in an inert atmosphere: one containing the sample and one empty; spectra were obtained of both.

Magnetic susceptibility measurements were carried out using a Quantum Design MPMS SQUID magnetometer, in the temperature range of 1.8−320 K and magnetic fields up to 2 T. The samples were sealed in gel capsules in an inert atmosphere, and transferred quickly to the magnetometer to reduce any possible exposure to the ambient.

Density functional calculations were performed in order to establish the electronic structure, site preference, and energetics of H in $Ba_3CrN_3H$. These were done using the experimentally determined lattice parameters, $a = 8.0270(2)$ Å and $c = 5.6240(1)$ Å. We used the general potential linearized augmented plane wave (LAPW) method,[19] as implemented in the WIEN2k code.[20] The total energy calculations and relaxation of the atomic coordinates were done using the Perdew−Burke−Ernzerhof (PBE) generalized gradient approximation (GGA).[21] Relativity was treated at a scalar relativistic level for the valence states. We relaxed all internal atomic coordinates by total energy minimization subject to symmetry. We used LAPW sphere radii of 2.3, 1.75, 1.4, and 1.4 bohr, for Ba, Cr, N, and H, respectively. The basis set, consisting of local orbitals for the semicore states plus LAPW functions up to a planewave cutoff determined by $R_{min}\,K_{max} = 7$, where $K_{max}$ is the planewave cutoff and $R_{min} = 1.4$ bohr, is the smallest sphere radius. The Brillouin zone was sampled using uniform meshes of at least 8 × 8 × 10.

## RESULTS AND DISCUSSIONS

Single crystals obtained by the described flux growth method are hexagonal prismatic, and have a green metallic color. They are very reactive and decompose rapidly in the ambient, rendering measurements time sensitive. The presence of anionic hydrogen and nitrogen is likely to be responsible. Other systems of the type $AE_3TN_3$ (AE = alkaline earth metal, T = transition metal) have also been reported to be unstable under ambient conditions.[22−24]

The structure of $Ba_3CrN_3H$ contains trigonal planar $[CrN_3]^{5-}$ units, arranged perpendicular to the $c$-axis, and $[HBa_6]^{11+}$ octahedra (Figure 1). Since there are three barium atoms per hydrogen atom, the charge based unit is therefore $[HBa_3]^{5+}$, balancing with the $[CrN_3]^{5-}$ unit. The barium framework comprises channel-like structures along the $c$-axis, in which the anionic hydrogen atom reside. These "channels" are face-shared, distorted octahedra with hydrogen in the center of each octahedron (Figure 1b). $HBa_6$ octahedra are also present in other hydrides: In both $Ba_3AlO_4H$[25,26] and $Ba_9In_4H$,[27] the octahedra form a three-dimensional framework of corner-shared octahedra, while in $Ba_{21}M_2O_5H_{12+x}$ (M = transition metals and metalloids), the face-sharing octahedra are arranged in a ring around a common central barium position.[28]

The Cr−N distance is 1.739(3) Å, shorter than the metal−nitrogen distances observed in $Ca_3CrN_3$: 1.766 Å for the shortest Cr−N bond and 2.388 Å for the shortest Ca−N bond.[24] The Ba−H distance in $Ba_3CrN_3H$ is 2.885 Å, longer than the values found in $BaH_2$, where distances range from 2.554 to 2.781 Å.[29] In $BaH_2$, however, the hydrogen atom is



DOI: 10.1021/acs.inorgchem.8b03367
Inorg. Chem. 2019, 58, 3302−3307

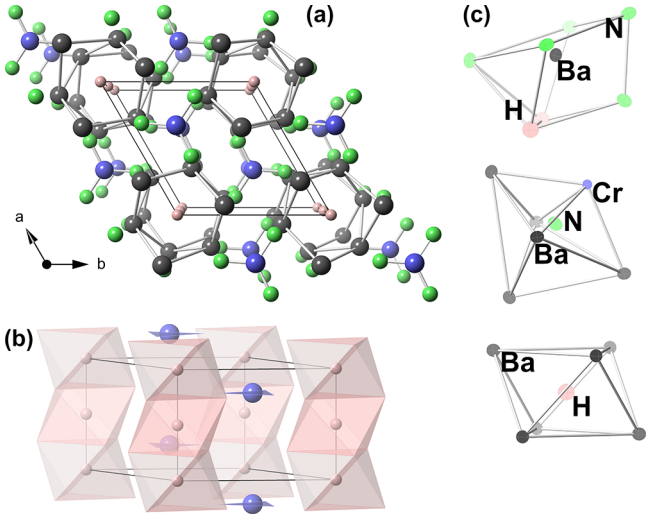


**Figure 1.** (a) Structure of $Ba_3CrN_3H$, viewed along the *c*-axis. Dark gray spheres are Ba, blue spheres are Cr, green spheres are N, and pink spheres are H. (b) View of the "channels" of face-shared Ba-octahedra with H in the center. (c) Atomic environments of Ba, N, and H displaying anisotropic displacement ellipsoids with 95% probability.

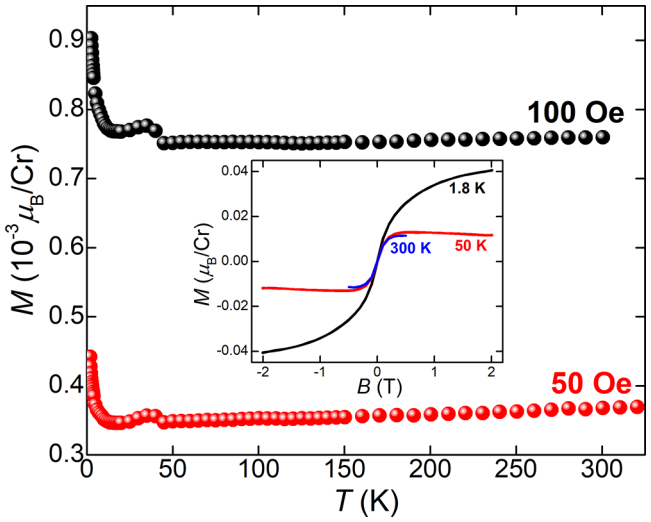


**Figure 2.** Magnetization as a function of temperature at 50 and 100 Oe for $Ba_3CrN_3H$. The moment is quite small (less than $10^{-3}$ $\mu_B$/Cr atom) and nearly constant across the measured temperature range. The bump around 40 K corresponds to the solidification of oxygen, followed by its antiferromagnetic transition. The low-temperature increase in magnetization is likely due to impurity phases. The inset displays magnetization as a function of applied field at 1.8, 50, and 300 K. Note the small moment of 0.04 $\mu_B$/Cr atom even at 1.8 K.

square pyramidal 5-coordinated and trigonal pyramidal 4-coordinated, whereas in $Ba_3CrN_3H$, the hydrogen is in the center of a trigonal distorted octahedron. Not taking into account the hydrogen, $AE_3TN_3$ compounds in this structure have been described in detail.[22−24] In this study, our bond valence sum (BVS) calculations and magnetic measurements gave us the first inclination that these structures were not yet fully understood. Assuming initially a charge-balanced $Ba_3CrN_3$, as already described in literature,[22] the BVS calculations yield 1.58 for the barium and 4.05 for the chromium, i.e., a strongly underbonded $Ba^{2+}$ and a strongly overbonded $Cr^{3+}$. These deviations were also noted by Barker et al. in a variety of $AE_3TN_3$ compounds,[22] where the high Cr valence was attributed to multiple Cr−N bonds and the low Ba valence to an overstretching of the Ba−N sublattice. Our EDS measurements confirmed that no other non-hydrogen elements besides nitrogen, chromium, and barium were present in the sample (hydrogen cannot be detected by EDS). Therefore, the BVS deviations could not be explained by the possibility of having other elements in the structure. With a BVS of 4.05, it is instead more likely that chromium is in the $Cr^{4+}$ configuration and not in the $Cr^{3+}$ configuration as suggested earlier. Furthermore, with chromium in trigonal planar geometry, $Cr^{4+}$ is expected to result in a nonmagnetic ground state. Indeed, our measurements of the magnetic moment across a wide temperature range yield a nearly constant and very low magnetic moment, less than $10^{-3}$ $\mu_B$/Cr atom; see Figure 2. The increase at low temperatures is likely to be due to impurity phases that form during the transfer of the sample from the inert atmosphere environment to the magnetometer. The feature around 40 K corresponds to the solidification of oxygen, followed by its antiferromagnetic transition Due to the small moments, even a small oxygen contamination manifests itself in the data. The inset to Figure 2 displays the magnetization as a function of applied field, and the low moment of ~0.04 $\mu_B$/Cr atom at 1.8 K is also likely a result of the aforementioned impurities. In order to charge-balance the compound, we suggest that this compound is in fact $Ba_3CrN_3H$ with chromium in a $Cr^{4+}$ configuration. Calculating bond valence sums for barium and chromium in this compound (with the hydrogen placed as suggested by the DFT calculations below), we obtain 1.90 and 4.05 (the Cr is not affected by the H which is over 4.8 Å away), respectively, i.e., BVS values in good agreement with the expected oxidation states.

The presence of hydrogen in $Ba_3CrN_3H$ was confirmed by NMR which looks at specific nuclei in a sample, based on a direct proportionality between the nucleus precessing frequency and applied magnetic field: $\omega = \gamma B$, where $\gamma$ is the gyromagnetic ratio ($\gamma/2\pi$ = 42.5774 MHz/T for $^1$H). Due to the ever-present hydrogens, we performed the experiment on two identical sample holders, one containing the actual sample and one containing nothing to unambiguously detect any hydrogen in the sample. The results are summarized in Figure 3, plotted as the NMR intensity against the shift relative to a reference frequency (given by the bare nucleus frequency, $\omega_0 = \gamma B_0$): $(\nu_{sample} - \nu_{reference})/\nu_{reference}$. It is clear that $Ba_3CrN_3H$ must contain hydrogen since the spectrum with a sample in the holder has an extra $^1$H peak when compared to the spectrum without a sample. In addition, this peak is much closer to the zero-shift frequency, corroborating that it is from the sample, since it was placed closer to the center of the magnetic field. Signals from probe parts would be further away since those parts are more off-center. Metal hydrides have a chemical shift range of approximately 0 to −60 ppm,[30,31] and the full $^1$H spectrum including any chemical shifts fits under the relatively wide peak (fwhm of about 155 ppm) we observe from the sample. Therefore, the large shift of the $^1$H peak (approximately −380 ppm) is due to the sample still being off-center, a consequence of the longer leads making it difficult placing the sample exactly in the center of the applied magnetic field.

While our NMR measurements confirmed the presence of hydrogen in $Ba_3CrN_3H$, the precise location could not be determined with the NMR setup. Instead, the location of the



DOI: 10.1021/acs.inorgchem.8b03367
Inorg. Chem. 2019, 58, 3302−3307

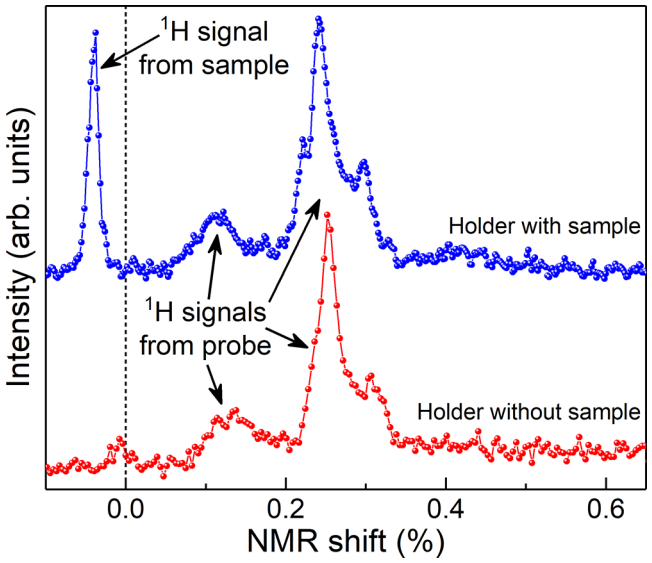


**Figure 3.** $^1$H NMR intensity vs the shift in %. The upper spectrum was obtained with a sample in the holder and the lower spectrum with no sample in the holder. The extra $^1$H peak close to zero shift confirms the presence of hydrogen in $Ba_3CrN_3H$.

hydrogen atom was determined by DFT calculations and the careful analysis of difference Fourier maps. Since X-ray diffraction using molybdenum radiation is not very sensitive to hydrogen, extensive DFT calculations to explore different hydrogen positions were carried out. There are two potential sites in the $Ba_3CrN_3H$ lattice that are large enough to contain anionic hydrogen, $H^-$, which is similar in size to the fluorine ion:[32] the 2b and 2c Wyckoff sites. Calculations were therefore carried out with H constrained to these two sites. We considered the cases of no H, H fully occupying the 2b sites, H fully occupying the 2c sites, and H fully occupying both the 2b and 2c sites. The $[CrN_3]^{5-}$ unit is charge balanced with Ba and anionic H. The two possible H sites are here denoted H1 and H2. H1 is the 2c site, which is between the Cr atoms along the *c*-axis (each H is coordinated by two Cr), and H2 is the 2b site, in the middle of the Ba cations, so that each H is coordinated by six Ba.

We begin with the energetics, taking the nonhydrided $Ba_3CrN_3$ as the energy zero. Relative to this, full occupation of the H1 site leads to an energy −15.3 eV/H, full occupation of the H2 site leads to an energy of −16.8 eV/H, and full occupation of both sites leads to an energy of −32.0 eV/f.u., i.e., −16.0 eV/H. For comparison, the total energy of one H in an $H_2$ molecule using the PBE GGA functional is −15.9 eV.[33] Thus the H2 (2b) site, with H coordinated by Ba, is very strongly preferred. Moreover, occupation of the H1 (2c) site, between the Cr, is highly disfavored relative to the $H_2$ molecule, and will not occur under ordinary synthesis conditions. However, the H2 site, coordinated by Ba is highly favored, with a binding enthalpy of −168 kJ/mol H2. This enthalpy is characteristic of a very stable hydride, comparable to $CaH_2$ or $SrH_2$, for example. Thus, we conclude that the stoichiometry $Ba_3CrN_3H$ is correct, with full occupation of the 2b site by hydrogen.

We now turn to the electronic structure based on occupation of the H2 (2b) site. We find that the compound is insulating and nonmagnetic. The nominal valence is $Cr^{4+}$, with two d electrons. The nominal valence of Cr without H, i.e., stoichiometry $Ba_3CrN_3$, is $Cr^{3+}$. We find that this stoichiometry is metallic. We did calculations for $Ba_3CrN_3H$ both with the PBE functional and also with the modified Becke−Johnson (mBJ) potential, constructed by Tran and Blaha.[34] This is a potential function that often gives band gaps in better accord with experiment than standard GGA density functionals.[34−36] We find an mBJ band gap of 2.1 eV, whereas the band gap calculated with the PBE functional is 1.4 eV.

The electronic density of states and projections of Cr d, H s, and N p character are shown in Figure 4, based on the mBJ

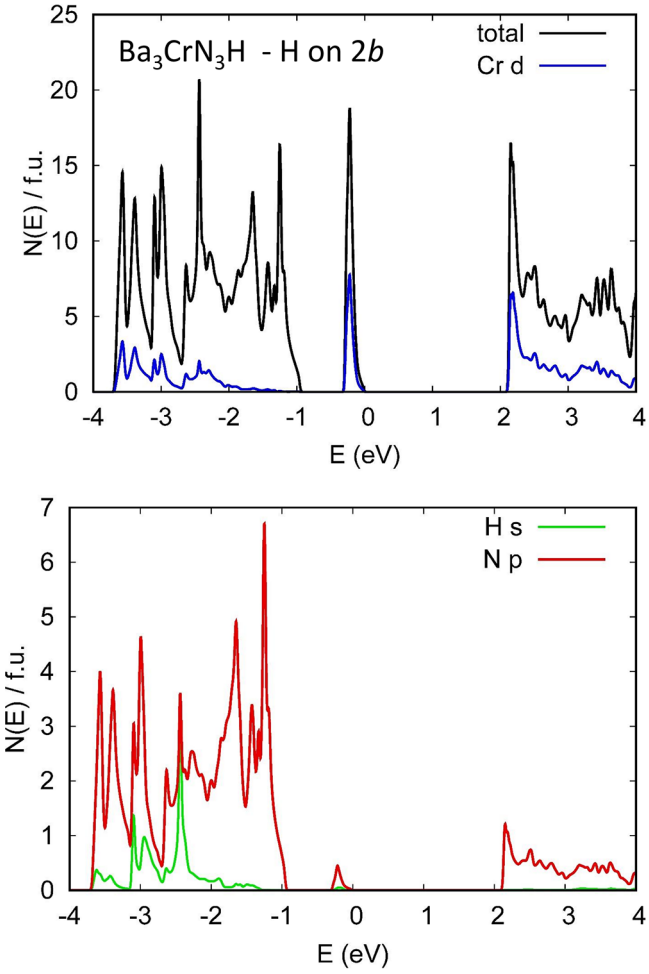


**Figure 4.** Top panel: Total density of states (DOS) of $Ba_3CrN_3H$ and projected DOS for Cr d electrons. Bottom panel: Projected DOS for H s and N p electrons.

results. The valence band is very narrow, and has Cr d character. The H s contribution is located in the energy range −3.5 to −2 eV, confirming that H is anionic in this compound. With a triangular planar coordination, the crystal field scheme has a nonbonding $d_{z^2}$ orbital, and higher lying $d_{xz}/d_{yz}$ and $d_{xy}/d_{x^2-y^2}$ manifolds. The very narrow valence bands come from the nonbonding Cr $d_{z^2}$ orbital (note that there are two Cr per unit cell, leading to two such bands). The other d orbitals form more dispersive conduction band states. The large crystal field gap is indicative of strong hybridization between the N p and Cr d states. This is also seen in the nominally N p derived bands between −4 and −1 eV, relative to the valence band maximum, which have quite significant Cr d contributions in the lower energy part. These correspond to the bonding states


DOI: 10.1021/acs.inorgchem.8b03367
*Inorg. Chem.* 2019, 58, 3302−3307

in correspondence with the antibonding character of the upper Cr d crystal field states comprising the conduction bands. It is this covalency that leads to the large crystal field splitting. In turn this explains the nonmagnetic character of the compound, since the nonbonding $d_{z^2}$ orbital is fully occupied, and the large crystal field gap disfavors moment formation.

The previously reported $Ba_3CrN_3$ by Barker et al.[22] has in essence the same structural features, while the unit cell constants differ. The unit cell given, with $a$ = 8.201 Å and $c$ = 5.497 Å, $c/a$ = 0.67, is significantly different from our values of $a$ = 8.027 Å and $c$ = 5.624 Å, $c/a$ = 0.70. The reported crystal growth does not show an obvious way that would introduce hydrogen. It is possible that hydrogen was introduced as impurities in the starting materials barium nitride, chromium nitride, or chromium metal. In fact, Barker et al.[22] note that oxygen impurities were probably introduced as part of the grinding of the starting materials. However, we have often identified crystals of $BaH_2$ in our flux growth, even if no hydride was added. We therefore surmise that Ba metal as received does contain small amounts of hydrogen, likely as a result of the reduction step in barium refining. As mentioned above, the structure by Barker et al. gives bond valence sums as 1.58 for Ba and as 4.1 for Cr, in essence strongly underbonded barium, and $Cr^{4+}$, in contrast to the valence of $Cr^{3+}$ given in the manuscript. The color of the crystals is green, as are our samples.[22] DFT calculations with the PBE functional relaxing the structure without hydrogen present do not reproduce the unit cell by Barker et al., whereas relaxation of the structure including hydrogen reproduces the values that are observed for $Ba_3CrN_3H$. Specifically, without H we obtain $a$ = 8.44 Å and $c$ = 5.44 Å, while with H we obtain $a$ = 8.08 Å and $c$ = 5.67 Å. Considering the typical errors in PBE calculations of ∼1% in lattice parameter, only the values with H are consistent with experiment. Since the crystal structure moieties in $Ba_3CrN_3$ are reasonable for $Cr^{4+}$ and within the range of distances expected, it is not clear if the reported structure does contain $Cr^{3+}$, which would render the phase metallic, not necessarily consistent with the color.

The unit cell of $Ba_3CrN_3H$ is quite different from the previously reported unit cell of $Ba_3CrN_3$,[22] but remarkably close to the reported unit cell of $Ba_3FeN_3$, with parameters $a$ = 8.014 Å, $c$ = 5.608 Å, and $c/a$ = 0.70.[23] However, the color reported for this phase is black, indicating metallic behavior. DFT calculations do show that $Ba_3FeN_3H$ is more stable than $Ba_3FeN_3$, and relaxed lattice parameters are close to the values reported. The PBE values of the lattice parameters of $Ba_3FeN_3H$ are $a$ = 7.96 Å and $c$ = 5.65 Å. For $Ba_3FeN_3$ without H, we obtain $a$ = 8.19 Å and $c$ = 5.48 Å. Furthermore, $Ba_3FeN_3H$ is determined as a metal as well. Since $Ba_3FeN_3$ also shows strong underbonding of the Ba, with a bond valence sum of 1.6 and the bond valence sum of 4.2 for iron indicates $Fe^{4+}$, it is conceivable that the $Ba_3FeN_3$ is actually $Ba_3FeN_3H$. Magnetic measurements could shed further light on the valence of the iron in this compound.

## CONCLUSIONS

The new nitride hydride $Ba_3CrN_3H$ has been obtained from a molten barium flux. The phase contains $[CrN_3]^{5-}$ trigonal planar units, with $Cr^{4+}$ ions. The two nonbonding chromium d-electrons are in the $d_{z^2}$ orbital, rendering the compound an insulator and nonmagnetic. DFT calculations show that the introduction of hydrogen increases the stability of $Ba_3CrN_3H$ over the nonhydride phase. In contrast to $Ca_3CrN_3$, the $[CrN_3]$ units in $Ba_3CrN_3H$ are not distorted and remain trigonal planar, consistent with the absence of a Jahn−Teller distortion for $Cr^{4+}$ in this trigonal coordination.

## ASSOCIATED CONTENT

### Accession Codes

CCDC 1874911 and 1879699 contain the supplementary crystallographic data for this paper. These data can be obtained free of charge via www.ccdc.cam.ac.uk/data_request/cif, or by emailing data_request@ccdc.cam.ac.uk, or by contacting The Cambridge Crystallographic Data Centre, 12 Union Road, Cambridge CB2 1EZ, UK; fax: +44 1223 336033.

## AUTHOR INFORMATION

### Corresponding Author

*E-mail: tigletbesara@missouristate.edu.

### ORCID

Tiglet Besara: 0000-0002-2143-2254

David J. Singh: 0000-0001-7750-1485

### Notes

The authors declare no competing financial interest.

## ACKNOWLEDGMENTS

Work at the University of Missouri is supported by the Department of Energy, Office of Science, Basic Energy Sciences, Award # DE-SC0019114. N.F., J.N., and T.S. acknowledge support from the National Science Foundation under NSF DMR-1606952. Part of the work was carried out at the National High Magnetic Field Laboratory, which is supported by the National Science Foundation under NSF DMR-1157490, DMR-1644779, and the State of Florida.

## REFERENCES

(1) Blaschkowski, B.; Schleid, T. Synthesis and crystal structure of the lithium strontium hydride nitride $LiSr_2H_2N$. *Z. Anorg. Allg. Chem.* **2007**, *633* (15), 2644−2648.

(2) Brice, J.-F.; Motte, J.-P.; Aubry, J. Preparation and properties of lithium hydridonitride, $Li_4NH$. *C. R. Seances Acad. Sci., Ser. C* **1973**, *276* (12), 1015−1016.

(3) Liu, D. M.; Liu, Q. Q.; Si, T. Z.; Zhang, Q. A. Synthesis and crystal structure of a novel nitride hydride $Sr_2LiNH_2$. *J. Alloys Compd.* **2010**, *495* (1), 272−274.

(4) Marx, R. Preparation and Crystal Structure of Lithium Nitride Hydride, $Li_4NH$, $Li_4ND$. *Z. Anorg. Allg. Chem.* **1997**, *623* (12), 1912−1916.

(5) Niewa, R.; Zherebtsov, D. A. Redetermination of the crystal structure of tetralithium mononitride monohydride, $Li_4NH$. *Z. Kristallogr. - New Cryst. Struct.* **2002**, *217* (1), 317−318.

(6) Brice, J.-F.; Motte, J.-P.; Courtois, A.; Protas, J.; Aubry, J. Structural study on $Ca_2NH$ by x-ray-diffraction, neutron-diffraction and proton nuclear magnetic-resonance in solid. *J. Solid State Chem.* **1976**, *17* (1−2), 135−142.

(7) Jacobs, H.; Niewa, R.; Sichla, T.; Tenten, A.; Zachwieja, U. Metal nitrogen compounds with unusual chemical bonding: Nitrides, imides, amides and ammine complexes. *J. Alloys Compd.* **1997**, *246* (1−2), 91−100.

(8) Bailey, M. S.; Obrovac, M. N.; Baillet, E.; Reynolds, T. K.; Zax, D. B.; DiSalvo, F. J. $Ca_6[Cr_2N_6]H$, the first quaternary nitride-hydride. *Inorg. Chem.* **2003**, *42* (18), 5572−5578.

(9) Dickman, M. J.; Schwartz, B. V. G.; Latturner, S. E. Low-dimensional nitridosilicates grown from Ca/Li flux: void metal $Ca_8In_2SiN_4$ and semiconductor $Ca_3SiN_3H$. *Inorg. Chem.* **2017**, *56* (15), 9361−9368.



DOI: 10.1021/acs.inorgchem.8b03367
*Inorg. Chem.* 2019, 58, 3302−3307

(10) Besara, T.; Ramirez, D.; Sun, J.; Whalen, J. B.; Tokumoto, T. D.; McGill, S. A.; Singh, D. J.; Siegrist, T. $Ba_2TeO$: A new layered oxytelluride. *J. Solid State Chem.* **2015**, *222*, 60−65.
(11) Besara, T.; Ramirez, D. C.; Sun, J. F.; Falb, N. W.; Lan, W. W.; Neu, J. N.; Whalen, J. B.; Singh, D. J.; Siegrist, T. Synthesis and crystal structure of the layered lanthanide oxychlorides $Ba_3Ln_2O_5Cl_2$. *Inorg. Chem.* **2018**, *57* (4), 1727−1734.
(12) Whalen, J. B.; Besara, T.; Vasquez, R.; Herrera, E.; Sun, J.; Ramirez, D.; Stillwell, R. L.; Tozer, S. W.; Tokumoto, T. D.; McGill, S. A.; Allen, J.; Davidson, M.; Siegrist, T. A new oxytelluride: perovskite and CsCl intergrowth in $Ba_3Yb_2O_5Te$. *J. Solid State Chem.* **2013**, *203*, 204−211.
(13) Falb, N. W.; Neu, J. N.; Besara, T.; Whalen, J. B.; Singh, D. J.; Siegrist, T. $Ba_3CrN_3H$: a new nitride-hydride with trigonal planar $Cr^{4+}$. **2018**, chemrxiv.7418429.v1. chemRxiv.org Preprint Server. https://chemrxiv.org/articles/Ba3CrN3H_A_New_Nitride-Hydride_with_Trigonal_Planar_Cr4_/7418429 (accessed December 12, 2018).
(14) *CrysAlisPro*, 171.39.46; Rigaku Corporation: Oxford, U.K., 2018.
(15) Betteridge, P. W.; Carruthers, J. R.; Cooper, R. I.; Prout, K.; Watkin, D. J. CRYSTALS version 12: software for guided crystal structure analysis. *J. Appl. Crystallogr.* **2003**, *36*, 1487.
(16) Palatinus, L.; Chapuis, G. *SUPERFLIP* - a computer program for the solution of crystal structures by charge flipping in arbitrary dimensions. *J. Appl. Crystallogr.* **2007**, *40*, 786−790.
(17) Bergerhoff, G.; Brown, I. D., Inorganic crystal structure database. In *Crystallographic Databases*; Allen, F. H.; Bergerhoff, G.; Sievers, R., Eds.; International Union of Crystallography: Chester, U.K., 1987; p 77.
(18) Groom, C. R.; Bruno, I. J.; Lightfoot, M. P.; Ward, S. C. The Cambridge Structural Database. *Acta Crystallogr., Sect. B: Struct. Sci., Cryst. Eng. Mater.* **2016**, *B72*, 171−179.
(19) Singh, D. J.; Nordström, L. *Planewaves, Pseudopotentials, and the LAPW Method*, 2nd ed.; Springer: Boston, MA, 2006; p XIII, 134.
(20) Blaha, P.; Schwarz, K.; Madsen, G.; Kvasnicka, D.; Luitz, J. *WIEN2k: An Augmented Plane Wave + Local Orbitals Program for Calculating Crystal Properties*; Technische Universität Wien, 2018.
(21) Perdew, J. P.; Burke, K.; Ernzerhof, M. Generalized gradient approximation made simple. *Phys. Rev. Lett.* **1996**, *77* (18), 3865−3868.
(22) Barker, M. G.; Begley, M. J.; Edwards, P. P.; Gregory, D. H.; Smith, S. E. Synthesis and crystal structures of the new ternary nitrides $Sr_3CrN_3$ and $Ba_3CrN_3$. *J. Chem. Soc., Dalton Trans.* **1996**, 1−5.
(23) Höhn, P.; Kniep, R.; Rabenau, A. $Ba_3[FeN_3]$: Ein neues Nitridoferrat(III) mit $[CO_3]^{2-}$-isosteren Anionen $[FeN_3]^{6-}$. *Z. Kristallogr.* **1991**, *196*, 153−158.
(24) Vennos, D. A.; Badding, M. E.; DiSalvo, F. J. Synthesis, structure, and properties of a new ternary metal nitride, $Ca_3CrN_3$. *Inorg. Chem.* **1990**, *29*, 4059−4062.
(25) Huang, B.; Corbett, J. D. $Ba_3AlO_4H$: synthesis and structure of a new hydrogen-stabilized phase. *J. Solid State Chem.* **1998**, *141* (2), 570−575.
(26) Zumdick, M.; Althoff, G.; Röhr, C. Barium oxoaluminate hydride. *Acta Crystallogr., Sect. C: Cryst. Struct. Commun.* **2001**, *57* (4), 339−340.
(27) Wendorff, M.; Scherer, H.; Röhr, C. Das Indid-Hydrid $Ba_9[In]_4[H]$: Synthese, Kristallstruktur, NMR-Spektroskopie, Chemische Bindung. *Z. Anorg. Allg. Chem.* **2010**, *636* (6), 1038−1044.
(28) Jehle, M.; Hoffmann, A.; Kohlmann, H.; Scherer, H.; Röhr, C. The 'sub' metallide oxide hydrides $Sr_{21}Si_2O_5H_{12+x}$ and $Ba_{21}M_2O_5H_{12+x}$ ($M$=Zn, Cd, Hg, In, Tl, Si, Ge, Sn, Pb, As, Sb, Bi). *J. Alloys Compd.* **2015**, *623*, 164−177.
(29) Ting, V. P.; Henry, P. F.; Kohlmann, H.; Wilson, C. C.; Weller, M. T. Structural isotope effects in metal hydrides and deuterides. *Phys. Chem. Chem. Phys.* **2010**, *12* (9), 2083−2088.
(30) Crabtree, R. H.; Segmuller, B. E.; Uriarte, R. J. T1's and proton NMR integration in metal hydride complexes. *Inorg. Chem.* **1985**, *24* (12), 1949−1950.
(31) Crabtree, R. H. *The Organometallic Chemistry of the Transition Metals*, 5th ed.; John Wiley & Sons: Hoboken, NJ, 2009.
(32) Shannon, R. D. Revised effective ionic radii and systematic studies of interatomic distances in halides and chalcogenides. *Acta Crystallogr., Sect. A: Cryst. Phys., Diffr., Theor. Gen. Crystallogr.* **1976**, *32*, 751−767.
(33) Ruzsinszky, A.; Perdew, J. P.; Csonka, G. I. Binding energy curves from nonempirical density functionals. I. Covalent bonds in closed-shell and radical molecules. *J. Phys. Chem. A* **2005**, *109* (48), 11006−11014.
(34) Tran, F.; Blaha, P. Accurate band gaps of semiconductors and insulators with a semilocal exchange-correlation potential. *Phys. Rev. Lett.* **2009**, *102* (22), 226401.
(35) Kim, Y.-S.; Marsman, M.; Kresse, G.; Tran, F.; Blaha, P. Towards efficient band structure and effective mass calculations for III-V direct band-gap semiconductors. *Phys. Rev. B: Condens. Matter Mater. Phys.* **2010**, *82* (20), 205212.
(36) Singh, D. J. Electronic structure calculations with the Tran-Blaha modified Becke-Johnson density functional. *Phys. Rev. B: Condens. Matter Mater. Phys.* **2010**, *82* (20), 205102.


DOI: 10.1021/acs.inorgchem.8b03367
*Inorg. Chem.* 2019, 58, 3302−3307